IEEE Access
Multidisciplinary : Rapid Review : Open Access Journal

Received August 28, 2019, accepted September 30, 2019, date of publication October 11, 2019, date of current version October 22, 2019.

Digital Object Identifier 10.1109/ACCESS.2019.2946728

Periodic Fixed-Frequency Staggered Line Leaky Wave Antenna With Wide-Range Beam Scanning Capacity

BIN XI[1], YUANXIN LI[2], (Member, IEEE), ZHIXI LIANG[2], (Member, IEEE), SHAOYONG ZHENG[2], (Senior Member, IEEE), ZENGPING CHEN[1], AND YUNLIANG LONG[2], (Senior Member, IEEE)

[1]School of Electronics and Communication Technology, Sun Yat-sen University, Guangzhou 510006, China
[2]School of Electronics and Information Technology, Sun Yat-sen University, Guangzhou 510006, China

Corresponding authors: Yuanxin Li (liyuanx@mail.sysu.edu.cn) and Zengping Chen (chenzengp@mail.sysu.edu.cn)

This work was supported in part by the Natural Science Foundation of China under Grant 61971453, and in part by the Natural Science Foundation of Guangdong Province under Grant 2015A030312010.

ABSTRACT A periodic fixed-frequency staggered line leaky wave antenna (LWA) with wide-range beam scanning capacity is proposed in this paper. The reconfigurable antenna is based on a periodic staggered line LWA. The dispersion and Bloch characteristics of the periodic antenna is analyzed by the Macro Cell Method (MCM). The open-stop band (OSB) of the antenna can be suppressed effectively using the relationship between widths of oblique feeding lines and stubs. The reconfigurable characteristic is achieved by switches and microstrip lines between the edge gaps of each unit cell. A "supercell" is established by combining several reconfigurable unit cells, and the state is controlled by connecting or disconnecting the edge gaps of each unit cell using switches. Fixed-frequency beam-scanning capacity is implemented due to different propagation constants in different supercell states. The prototyped reconfigurable antenna can scan the beam between 130° and 54° at 4.5 GHz.

INDEX TERMS Periodic, LWA, reconfigurable, broadside radiation, macrocell.

I. INTRODUCTION

The microstrip leaky wave antenna (MLWA) has attracted significant research attention since being developed in 1979 [1] due to unique advantages, such as simple structure, low profile, and beam-scanning capacity in the H-plane [2], [3]. MLWA designs with backward-to-forward beam-scanning capacity using the periodic waveguide structure have been reported [4]. Various periodic antenna designs have been developed, such as the periodic half-width MLWA [5], periodic triangle truncated DSPSL-based antenna [6], and a new type of circularly polarized printed periodic LWA structure [7].

However, the present of an open-stop band (OSB) limits the radiation of periodic structures in the broadside direction, causing a degraded radiation pattern and high return loss [8], [9]. Several methods have been proposed to suppress the OSB in periodic structures. The balanced condition has been confirmed as a useful condition in designing the CRLH LWA to reduce the OSB [10]. An OSB elimination technique, equal phase shift condition, for a class of periodic LWA with two types of uniform transmission lines in alternatively cascading arrangement is proposed in [11].

The beam scanning capacity of the MLWA depends on variations in frequency [12]. Most communication systems operate in the predefined frequency; thus, scanning at a selected frequency is highly desirable [13], [14]. One method is to manipulate the phase constant of the leaky micro-slotline using reactive loading across the slotline [15]. Another method involves changing the feed position along an edge, with a main beam scan from 50° to 80° at 1.12 GHz [16]. A novel fixed-frequency electronically steerable 1-D LWA based on a tunable high impedance surface was presented in [17] with a scanning range of 21° at 5.6 GHz. A radiation pattern-reconfigurable LWA based on SIW structure is presented in [18], and the beam can be steered from 45 to 68 at 5.2 GHz. Another method involves implementing a reconfigurable antenna using binary switches, and the antenna can

The associate editor coordinating the review of this manuscript and approving it for publication was Dimitris Anagnostou.

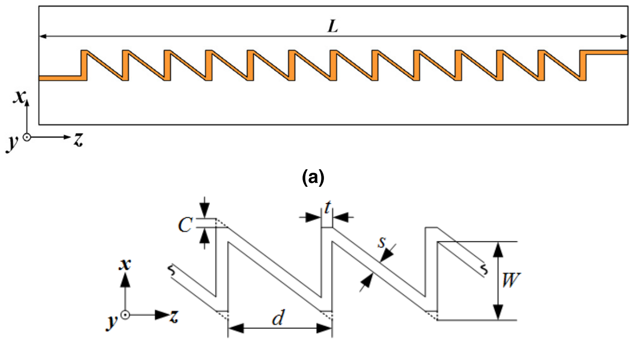

FIGURE 1. Periodic staggered line LWA. (a) Top view; (b) Detail view.

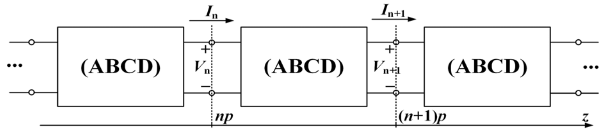

FIGURE 2. Equivalent network with minimal periodic *p* of a 1-D periodic structure.

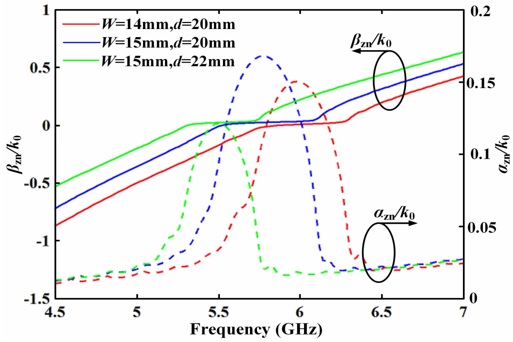

FIGURE 3. The normalized wavenumbers of the periodic LWA.

scan the main beam between 31° and 60° at 6 GHz [19]. A new double-gap capacitor technique to control the radiation of periodic half-width MLWAs at a fixed frequency was presented in [20]. A beam-scanning LWA based on the half-mode bent corrugated SIW structure was proposed in [21], and the antenna achieves a scan-angle range of 25° at 5.8 GHz.

A periodic fixed-frequency LWA with wide-range beam scanning capacity is outlined herein. The structure is based on a periodic staggered line antenna. In Section II, the dispersion and Bloch characteristics of the periodic antenna are analyzed by MCM. A method for suppressing the OSB is obtained, and the antenna performance is confirmed with measured results. In Section III, the reconfigurable characteristics and implementation of the fixed-frequency beam scanning capacity are discussed. In Section IV, a prototype of the proposed periodic fixed-frequency antenna based on periodic staggered line LWA is presented. In Section V, measured results of the proposed reconfigurable structure in selected ''supercell'' states are shown.

II. PERIODIC LEAKY WAVE ANTENNA

A. DISPERSION CURVES

A periodic staggered line leaky wave antenna, shown in Fig. 1, is proposed. This periodic staggered line LWA consists of a series of stubs and oblique feeding lines, which are periodically and interlaced distributed along the wave propagation direction.

The transversal spacing is W and the length of unit cell is p, which is also the periodic of the proposed structure. The propagation wavenumber k_{zn} is mainly determined by the parameters above. To achieve better impedance matching and ease of testing, a piece of 50-Ω microstrip transmission line is attached on each side of the entire LWA. The excitation signal is input to the left side of the antenna, and the load is connected to the right side for absorbing the remaining electromagnetic wave. The proposed periodic antenna possesses a backward-to-forward scanning capacity.

The periodic structure can be modeled as an infinite cascade of identical networks [22], and the equivalent network with minimal periodic p is shown in Fig. 2. Each unit cell is characterized through its *ABCD* matrix:

$$\begin{pmatrix} V_{n+1} \\ I_{n+1} \end{pmatrix} = \begin{pmatrix} A & B \\ C & D \end{pmatrix} \begin{pmatrix} V_n \\ I_n \end{pmatrix}. \tag{1}$$

The *ABCD* matrix can be calculated through S-parameters using the conversion formulas.

The method of single unit (Single Cell Method, SCM) assumes that the dispersion behavior of the isolated cell remains the same when it is placed within the periodic structure [23]. But this is not the case since electromagnetic interactions between unit cells. In order to effectively take into account mutual coupling effects and sufficiently dilute edge aperiodic effects, a new network, ''macrocell'', made by N adjacent single cells (MCM) is used to analyze the dispersion characteristics [24].

A macrocell is modeled through the matrix $(ABCD)_N$, where the distance between the network is Np, and an estimate of the wavenumbers $k_{z,\mathrm{i}}$ can be obtained as follows [25]:

$$\begin{aligned} k_{z,i} &= \frac{j}{Np}\ln(\lambda_{N,i}) \\ &= -\frac{Arg(\lambda_{N,i})}{Np} - \frac{2\pi m}{Np} + j\frac{\ln(\lambda_{N,i})}{Np} \\ &= \beta_i - j\alpha_i, \end{aligned} \tag{2}$$

where $\lambda_{\mathrm{N,i}}$ ($i = 1,2$) are eigenvalues of the matrix $(ABCD)_N$. The function $\ln(\cdot)$ is the logarithm, whose imaginary part is defined up to an integer multiple of 2π, and $\mathrm{Arg}(\cdot)$ is the principle argument of a complex number in $(-\pi, \pi]$.

Fig. 3 shows the normalized phase constant β_{zn}/k_0 and attenuation constant α_{zn}/k_0 of the periodic structure with different parameters, which are calculated by MCM. The S-parameters used for calculation are extracted using *Anosoft HFSS*. The operating band shifts toward the lower frequency as the antenna width W increases. The spacing d affects

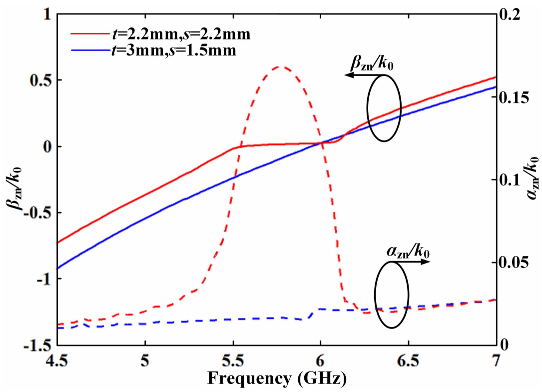

FIGURE 4. The normalized propagation wavenumbers of the periodic LWA with different t/s.

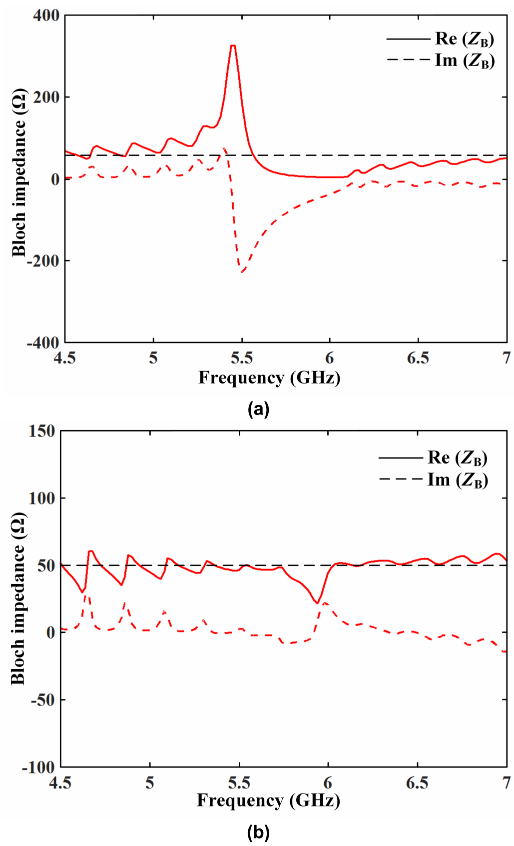

FIGURE 5. The Bloch propagation Z_B of the periodic LWA with different t/s. (a) $t = 2.2$mm, $s = 2.2$mm; (b) $t = 3$mm, $s = 1.5$mm.

antenna performance as a periodic factor, and this effect is reflected in shifts of the operating band toward the lower frequency as the spacing increases.

The open-stop band (OSB) effect is represented by the bump of the normalized attenuation constant curve, shown in Fig. 3. The presence of the OSB affects the continuous scanning of main beam seriously, and the elimination of the OSB is necessary.

B. OSB ELIMINATION

The proposed periodic LWA consists of stubs and oblique feeding lines. The oblique feeding line mainly realizes the energy transmission, and leakage of electromagnetic waves is achieved by stubs mainly.

The suppression of the OSB can be casted in terms of a linear curve of the normalized phase constant and a flat curve of the normalized attenuation constant [26]. The unit cell of the proposed periodic structure consists of a stub and an oblique feeding line. The impedance of unit cell can be adjusted by changing widths of the stub (t) and the oblique feeding line (s). By changing parameters of the unit cell, the impedance can be made almost equal to $Z_0 = 50\ \Omega$ at the broadside frequency. The OSB in this periodic structure is related to the ratio of t/s (t and s denote the width of stubs and feeding lines, respectively).

The normalized propagation wavenumbers of the antenna with different t/s ($W = 15$mm, $d = 20$mm) are shown in Fig. 4. The wavenumbers given in Fig. 4, where $t/s = 1$ ($t = s = 2.2$mm) and $t/s = 2$ ($t = 3$mm, $s = 1.5$mm) respectively, are calculated by (3). From these results we observe that there is no OSB effect in the case of $t/s = 2$. Near $\beta_{zn}/k_0 = 0$ frequency, the normalized phase constant is linear, and the normalized attenuation constant has a small swing, but is basically constant.

The relevant Bloch impedance of the proposed periodic LWA is then analyzed by MCM. The elimination of the OSB is manifested by ensuring that an almost real, non-zero Bloch impedance Z_B is obtained at broadside. From Fig. 5(a), the OSB effects are evident near the broadside frequencies ($t = s = 2.2$mm) clearly. The Bloch impedance, shown in Fig. 5(b) is real and flat essentially, with a small reactive bump near 6 GHz, thus confirming the elimination of OSB.

Fig. 6 shows the comparison of the radiation patterns around the broadside direction in above two cases. From Fig. 6(b), the main beam scans continuously through the broadside without gain degradation., which proves that the optimization technique is effective.

C. MEASURED RESULTS

The prototype of the periodic staggered line LWA is shown in Fig. 7.

The measured y-z plane radiation patterns are depicted in Fig. 8. With the increase of frequency, the main beam continuously steers from backward to forward through broadside. Experimental results show that the main beam scans from 146° to 40° when the frequency increases from 4.5 GHz to 7.9 GHz.

The simulated and measured results of main beam angle and normalized attenuation constants α_{zn}/k_0 are shown in Fig. 9. And the results are matched well. The measured reflection coefficient and gain are displayed in Fig. 10. The S-parameter (S_{11}) in the operating band is less than -10 dB, indicating a strong match. The measured gain is essentially constant as the beam is scanned through the

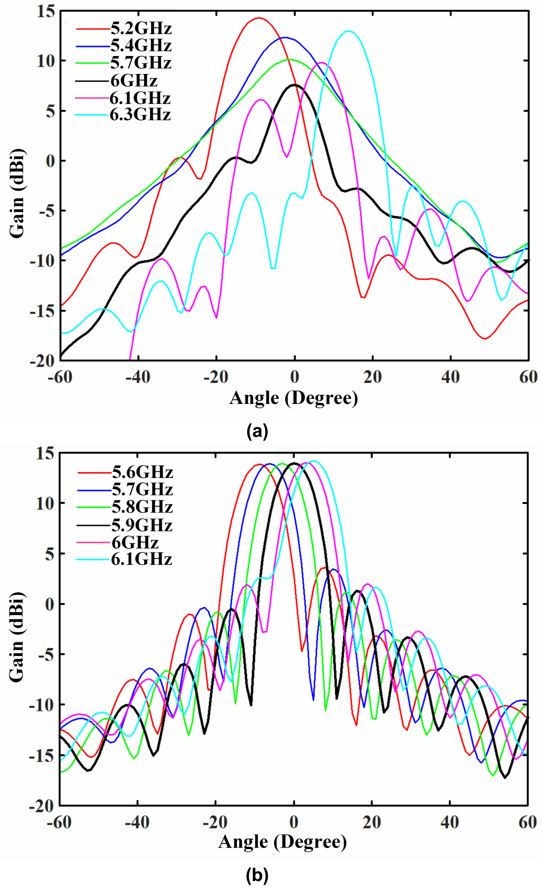

FIGURE 6. Simulated gain versus angle in different frequencies in (a) $t = 2.2$mm, $s = 2.2$mm; (b) $t = 3$mm, $s = 1.5$mm.

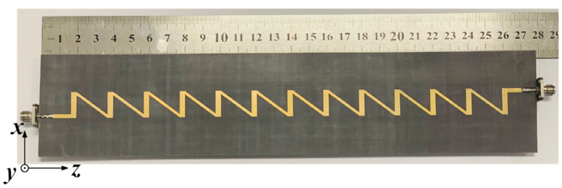

FIGURE 7. Prototype of periodic staggered line antenna.

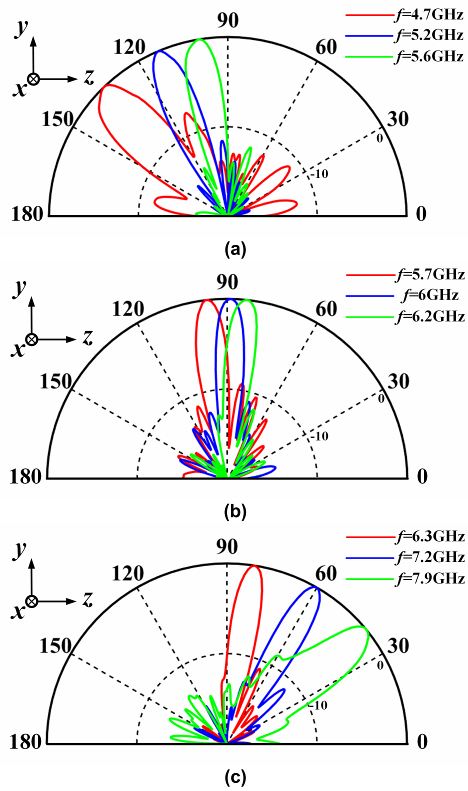

FIGURE 8. Measured radiation patterns of proposed periodic antenna.

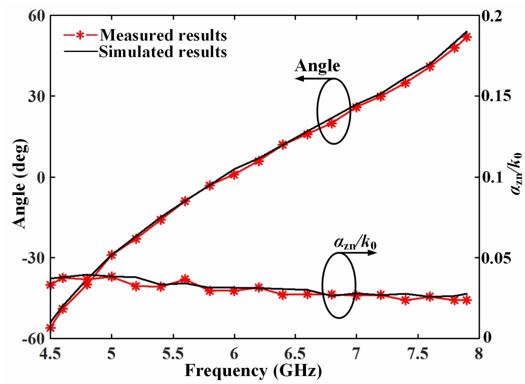

FIGURE 9. The main beam direction and normalized attenuation constant of the periodic antenna.

broadside direction, and its above 6.5 dBi in all operating band.

III. IMPLEMENTATION OF FIXED-FREQUENCY SCANNING

As discussed in Section II, a periodic staggered line LWA has been developed. Based on the results, a periodic reconfigurable LWA using switches and microstrip lines between the edge gaps of each unit cell is proposed.

A. RECONFIGURABLE CHARACTERISTICS

The configuration of the proposed periodic reconfigurable antenna is shown in Fig. 11. The whole length of the substrate is 278 mm ($4.23\lambda_0$), where λ_0 is the free-space wavelength at 4.5 GHz. Reconfigurable characteristics of the antenna can be achieved by connecting or disconnecting the edge gaps using switches and microstrip lines.

To help understand the reconfigurable characteristics of the proposed antenna, the concept of creating a "supercell" consisting of multiple unit cells is created here. The number of unit cells in a supercell is variable, and the state of each supercell can be changed by controlled switches between the edge gaps. Each switch is in one of two states, "ON" or "OFF", as shown in Fig. 11(b). For ease of analysis, these switch states are denoted as "1" and "0", respectively.

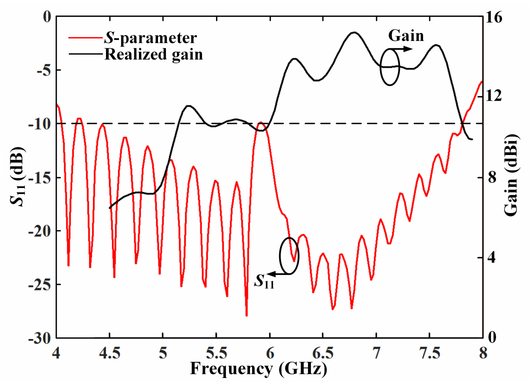

FIGURE 10. Measure S-parameter and gain of the periodic antenna.

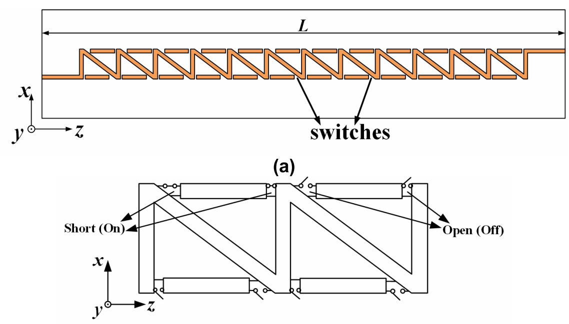

FIGURE 11. Configuration of proposed fixed-frequency antenna.(a) Top view; (b) Switch states ("On" and "Off").

B. FIXED-FREQUENCY SCANNING

Here, we use the symbol $\mathrm{S}i(j)$ to represent the supercell, where i denotes the number of unit cells in a supercell (ith-order), and j denotes the jth state of the ith-order supercell. The radiation characteristics of the periodic antenna are determined by the complex propagation constant k_{zn}. The direction $\theta_{\mathrm{S}i(j)}$ of the main beam is defined by the normalized phase constant $\beta_{\mathrm{zn}(\mathrm{S}i(j))}/k_0$ [27]:

$$\theta_{Si(j)} = \frac{\pi}{2} - \sin^{-1}\left(\frac{\beta_{zn(Si(j))}}{k_0} - \frac{2n\pi}{p_{Si(j)}}\right). \tag{3}$$

In conventional periodic structure, the periodic spacing $p_{\mathrm{Si(j)}}$ is always constant, and the implementation of beam-scanning capacity is based on the relationship between the normalized phase constant $\beta_{\mathrm{zn}(\mathrm{S}i(j))}/k_0$ and operating frequency f. But the fixed-frequency beam-scanning capacity here is not only related to $\beta_{\mathrm{zn}(\mathrm{S}i(j))}/k_0$, but also to $p_{\mathrm{S}i(j)}$. Wherein, the periodic spacing $p_{\mathrm{S}i(j)}$ is associated with the number of unit cells in a supercell:

$$p_{Si(j)} = ip. \tag{4}$$

The state and number of unit cells in a supercell are controlled by switches and microstrip lines between the edge gaps. The reconfigurable characteristics of the proposed structure is reflected by the transition of the supercell state. The implementation of fixed-frequency beam-scanning capacity has two methods: The first method is to control the periodic spacing $p_{\mathrm{S}i(j)}$, that is, to change $p_{\mathrm{S}i(j)}$ via the number of unit cells (i) in a supercell, then the direction $\theta_{\mathrm{S}i(j)}$ of main beam changes accordingly. The second method is that the number of unit cells remains constant at the selected frequency, the supercell state is controlled by switches. The normalized phase constant $\beta_{\mathrm{zn}(\mathrm{S}i(j))}/k_0$ at the given frequency is affected by the transition of supercell state ($Si(j)$), and the direction $\theta_S i(j)$ of main beam shifts.

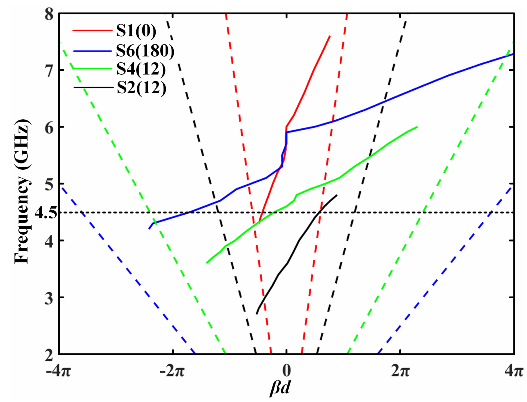

FIGURE 12. Dispersion diagrams in different supercell states.

Based on the description of the fixed-frequency scanning mechanism, each structure consisting of different supercell states has a corresponding propagation constant $k_{\mathrm{zn}(\mathrm{S}i(j))}$ at a given frequency. Therefore, the radiation beam can be steered correspondingly at given frequency.

The dispersion characteristics of the periodic staggered line LWA is analyzed with MCM in Section II(A). MCM will continue to be used here to analyze the dispersion characteristics of the proposed reconfigurable antenna in different supercell states.

The S-parameters used in the "macrocell" method for dispersion characteristic analysis are extracted by *Ansoft HFSS*. Dispersion diagrams of the proposed reconfigurable structure in different supercell states are displayed in Fig. 12, and all selected structures are in the leakage region. Different propagation constants $k_{\mathrm{zn}(\mathrm{S}i(j))}$ are gotten in different supercell states at 4.5 GHz, and the fixed-frequency scanning capacity is achieved.

C. VERIFICATION

The reconfigurable characteristics and fixed-frequency scanning of the antenna are verified by *Ansoft HFSS*. The supercell has $2^2 = 4$ states (00, 01, 10, and 11) when a supercell consists of only one-unit cell. Correspondingly, a supercell (N unit cells) can be considered a multistate electromagnetic element with $2^{2\mathrm{N}}$ states. For a supercell containing multiple unit cells, it is possible to find one or more supercells containing a small number of unit cells with identical characteristics. For example, the properties of 10 (S1(2)) and 1010 (S2(10)) are identical.

TABLE 1. Beam angles corresponding to supercell states.

Supercell states	Switches configuration	S_{11} (dB)	Beam direction (θ)	3dB Beam-width	Gain (dBi)
S1(0)	000000000000000000000000	-34.4434	135º	17.61º	10.06
S4(101)	011001010110010101100101	-14.4004	130º	23.54º	7.9
S6(39)	000000100111000000100111	-19.1268	119º	15.37º	7.52
S3(34)	100010100010100010100010	-16.3353	109º	20.14º	9.07
S6(144)	000010010000000010010000	-31.5998	106º	12.17º	8.93
S4(9)	000010010000100100001001	-19.767	97º	13º	9.08
S4(12)	000011000000110000001100	-16.6451	95º	12.14º	8.33
S6(34)	000000100010000000100010	-10.6539	90º	17.14º	9.42
S6(2313)	100100001001100100001001	-32.2192	88º	11.87º	8.86
S3(12)	001100001100001100001100	-12.9502	85º	13.13º	10.19
S6(204)	000011001100000011001100	-21.7938	82º	12.21º	7.73
S4(81)	010100010101000101010001	-11.0258	77º	29.7º	8.04
S6(721)	001011010001001011010001	-11.3182	66º	17.18º	9.58
S4(147)	100100111001001110010011	-12.9324	63º	14.53º	8.05
S2(12)	110011001100110011001100	-18.8978	60º	15.56º	7.62

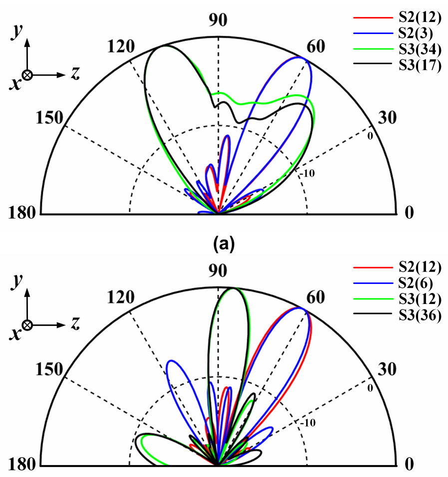

(a)
(b)

FIGURE 13. Main beams in different supercell states.

TABLE 2. parameters of proposed antenna.

Symbol	Parameter	Size(mm)
W	Width of antenna	15
d	Structural spacing	20
s	Width of oblique feeding line	2.2
t	Width of stub	2.2
L	Whole antenna length	278

The radiation beams point in the same direction when two supercell states are rotationally symmetric. As shown in Fig. 13(a), the man beams of 1100 (S2(12)) and 0011 (S2(3)) are pointing at 61° simultaneously; the structures of 010001 (S3(17)) and 100010 (S3(34)) have the same radiation direction, pointing at 109°. Furthermore, not all supercell states provide a unique beam direction. The main beams of 0110 (S2(6)), 1100 (S2(12)) and 001100 (S3(12)), 100100 (S3(36)), indicated in Fig. 13(b), point at 61° and 85°, respectively.

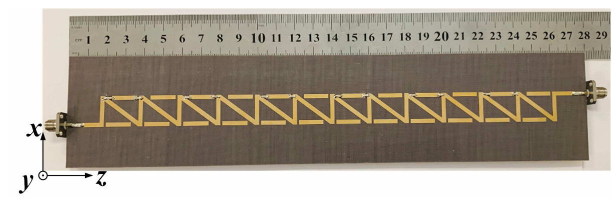

FIGURE 14. Prototype of the fixed-frequency antenna.

In summary, many supercell states provide the same direction at the selected frequency. In this case, the most appropriate structure should be chosen according to other characteristic parameters (e.g., gain and S-parameter). A fixed-frequency scanning range of 135° to 60° at 4.5 GHz is achieved in this antenna design. Details of the fixed-frequency scanning are listed in Table 1; only some results are shown here.

IV. ANTENNA DESIGH

The proposed periodic reconfigurable antenna is based on the front periodic staggered line LWA. A top view of the reconfigurable antenna prototype is shown in Fig. 14. The antenna is fabricated on a substrate with dielectric constant

TABLE 3. Simulated and measured results in selected supercell states at 4.5 GHz.

Supercell state	S_{11} (dB)		Beam direction (θ)		Gain (dBi)		3dB Beam-width		Side-lobe level (dB)	
	Simulated	Measured	Simulated	Measured	Simulated	Measured	Simulated	Measured	Simulated	Measured
S1(0)	-34.2316	-11.4562	135°	130°	10.06	9.04	17.61°	17.65°	-21.41	-20.14
S6(180)	-11.6509	-10.6677	118°	118°	9.46	8.17	14.09°	14.27°	-19.34	-19.3
S4(12)	-16.6451	-11.0064	94°	98°	8.33	7.07	12.14°	12.06°	-18.07	-18.78
S6(721)	-11.3182	-10.2584	66°	66°	9.58	8.22	17.18°	16.24°	-21.24	-22.7
S2(12)	-18.8978	-12.6152	60°	54°	7.62	6.15	15.56°	15.32°	-21.71	-27.56

TABLE 4. Comparison between the characteristics.

Antenna	Operating frequency (GHz)	Size (λ_0)	S_{11}<-10dB	Maximum Gain(dBi)	Scanning Range
[13]	4.5	3.6	Not all	5.8	131°~59°(72°)
[15]	4	2.93	No	-	13°
[16]	1.12	1.18	-	-	80°~50°(30°)
[17]	5.6	5	Yes	15	81°~60°(21°)
[18]	5.2	6.1	Yes	5.53	44°~22°(22°)
[19]	6	5.32	Yes	12.9	59°~30°(29°)
This Work	4.5	4.23	Yes	9.04	**130°~54°(76°)**

$\varepsilon_r = 2.55$, dielectric loss tangent $\tan\delta = 0.005$, and thickness $h = 0.8$ mm. All antenna parameters are listed in Table 2.

In order to facilitate the control of "supercell" states, diodes are introduced as switches here. When the diode is cut off, it is equivalent to the "0" (OFF) state of the switch. Conversely, the conduction of diode is equivalent to the "1" (ON) state. The edge gaps can be connected or disconnected by controlling the bias state of diode, and the "supercell" state is controlled accordingly. The selected diode model is HSMS-286F-TR1G, and its operating band includes 915 MHz $\sim$ 5.8 GHz.

Five supercell states S1(0) (00), S6(180) (000010110100), S4(12) (00001100), S6(721) (001011010001), and S2(12) (1100) are selected to observe beam scanning at 4.5GHz. The minimum and maximum beam angles are given for S1(0) (00) and S2(12) (1100), respectively.

V. MEASURED RESULTS

The proposed periodic reconfigurable antenna prototype in selected states is measured in the far-field condition.

A. S-PARAMETERS AND GAIN

Reflection coefficients and measured gain of the antenna prototype in selected states are measured. The measured S-parameters (S_{11}) and gains at 4.5 GHz are presented in Table 3. Due to the influence of the diode (switch) and the machining accuracy, there is a certain difference between the measured results and simulated results.

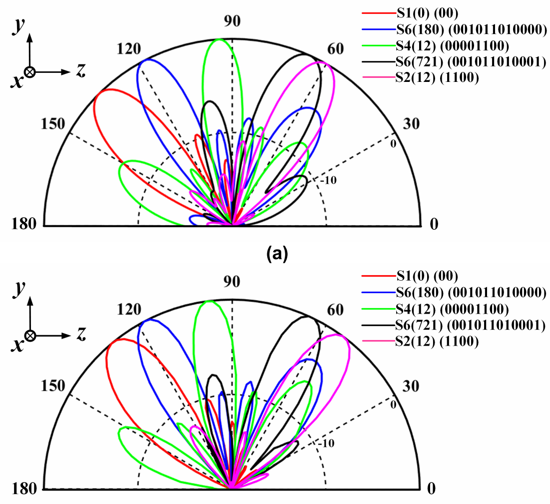

FIGURE 15. Simulated and measured radiation patterns of fixed-frequency antenna in selected supercell states. (a) Simulated results; (b) Measured results.

B. RADIATION PATTERNS

Measured and simulated y-z plane radiation patterns of the periodic reconfigurable antenna in selected states are shown in Fig. 15.

From simulated radiation patterns, indicated in Fig. 15(a), the main beam is directed at 135° in the state of S1(0) (00).

In other selected states, the main beam points to 118°, 94°, 66°, and 60°, respectively. Accordingly, as shown in Fig. 15(b), the measured beams are directed at 130°, 118°, 98°, 66°, and 54° in selected states, respectively.

The measured and simulated results are essentially the same. The measured results further substantiate the feasibility of the proposed fixed-frequency reconfigurable antenna. The main beam is gradually scanned at 4.5 GHz as the supercell state changes. The measured results reveal that the main beam can be steered between 130° and 54°.

A comparison between the characteristics of the proposed antenna and some of the recent fixed-frequency antenna are listed into Table 4. From Table 4, the advantage of wide-range beam scanning capacity is obvious compared with the existing fixed-frequency antennas.

VI. CONCLUSION

A periodic fixed-frequency staggered line leaky wave antenna with wide-range beam scanning capacity is presented in this paper. The proposed reconfigurable antenna is based on a periodic staggered line LWA. The MCM is used to analyze the characteristics of the periodic structure. Besides, a method for eliminating OSB of the periodic antenna is obtained, and the validity is verified by the measured results.

A multistate ''supercell'' approach is developed to analyze the proposed reconfigurable antenna. The supercell state can be altered by connecting or disconnecting edge gaps using switches and microstrip lines. The fixed-frequency scanning capacity is realized via changes the number of periodic units in a supercell and the supercell state. Simulation analyses and experimental measurements validate the results. The measured scanning range of the antenna prototype is 76° at 4.5 GHz.

REFERENCES

[1] W. Menzel, ''A new travelling-wave antenna in microstrip,'' *Arch. Elek Ubertragung.*, vol. 33, pp. 137–140, Apr. 1979.

[2] D. R. Jackson, C. Caloz, and T. Itoh, ''Leaky-wave antennas,'' *Proc. IEEE*, vol. 100, no. 7, pp. 2194–2206, Jul. 2012.

[3] S. Ge, Q. Zhang, C.-Y. Chiu, Y. Chen, and R. D. Murch, ''Single-side-scanning surface waveguide leaky-wave antenna using spoof surface plasmon excitation,'' *IEEE Access*, vol. 6, pp. 66020–66029, 2018.

[4] D. K. Karmokar and K. P. Esselle, ''Periodic u-slot-loaded dual-band half-width microstrip leaky-wave antennas for forward and backward beam scanning,'' *IEEE Trans. Antennas Propag.*, vol. 63, no. 12, pp. 5372–5381, Dec. 2015.

[5] Y. Li, Q. Xue, E. K.-N. Yung, and Y. Long, ''The periodic half-width microstrip leaky-wave antenna with a backward to forward scanning capability,'' *IEEE Trans. Antennas Propag.*, vol. 58, no. 3, pp. 963–966, Mar. 2010.

[6] D. Ye, Y. Li, Z. Liang, J. Liu, S. Zheng, and Y. Long, ''Periodic triangle-truncated DSPSL-based antenna with backfire to endfire beam-scanning capacity,'' *IEEE Trans. Antennas Propag.*, vol. 65, no. 2, pp. 845–849, Feb. 2017.

[7] M. H. Rahmani and D. Deslandes, ''Backward to forward scanning periodic leaky-wave antenna with wide scanning range,'' *IEEE Trans. Antennas Propag.*, vol. 65, no. 7, pp. 3326–3335, Jul. 2017.

[8] S. Paulotto, P. Baccarelli, F. Frezza, and D. R. Jackson, ''Full-wave modal dispersion analysis and broadside optimization for a class of microstrip CRLH leaky-wave antennas,'' *IEEE Trans. Microw. Theory Techn.*, vol. 56, no. 12, pp. 2826–2837, Dec. 2008.

[9] D. K. Karmokar, S.-L. Chen, T. S. Bird, and Y. J. Guo, ''Single-layer multi-via loaded CRLH leaky-wave antennas for wide-angle beam scanning with consistent gain,'' *IEEE Antennas Wireless Propag. Lett.*, vol. 18, no. 2, pp. 313–317, Feb. 2019.

[10] J. S. Gomez-Diaz, D. Canete-Rebenaque, and A. Alvarez-Melcon, ''A simple CRLH LWA circuit condition for constant radiation rate,'' *IEEE Antennas Wireless Propag. Lett.*, vol. 10, pp. 29–32, 2011.

[11] D. Xie, J. Wen, L. Zhu, X. Liu, H. Guo, H. Bu, X. M. Yang, and C. R. Liu, ''Uniform periodic leaky-wave antennas with eliminated open stopbands,'' *IEEE Antennas Wireless Propag. Lett.*, vol. 16, pp. 2110–2113, 2017.

[12] D. Sánchez-Escuderos, M. Ferrando-Bataller, J. I. Herranz, and M. Cabedo-Fabrés, ''Periodic leaky-wave antenna on planar Goubau line at millimeter-wave frequencies,'' *IEEE Antennas Wireless Propag. Lett.*, vol. 12, pp. 1006–1009, 2013.

[13] K. Chen, Y. H. Zhang, S. Y. He, H. T. Chen, and G. Q. Zhu, ''An electronically controlled leaky-wave antenna based on corrugated SIW structure with fixed-frequency beam scanning,'' *IEEE Antennas Wireless Propag. Lett.*, vol. 18, no. 3, pp. 551–555, Mar. 2019.

[14] L. Ge, M. Li, Y. Li, H. Wong, and K.-M. Luk, ''Linearly polarized and circularly polarized wideband dipole antennas with reconfigurable beam direction,'' *IEEE Trans. Antennas Propag.*, vol. 66, no. 4, pp. 1747–1755, Apr. 2018.

[15] C.-C. Chen and C. K. C. Tzuang, ''Phase-shifterless beam-steering micro-slotline antenna,'' *Electron. Lett.*, vol. 38, no. 8, pp. 354–355, Apr. 2002.

[16] Y. Li and Y. Long, ''Frequency-fixed beam-scanning microstrip leaky-wave antenna with multi-terminals,'' *Electron. Lett.*, vol. 42, no. 1, pp. 7–11, Jan. 2006.

[17] R. Guzman-Quiros, J. L. Gomez-Tornero, A. R. Weily, and Y. J. Guo, ''Electronically steerable 1-D Fabry–Perot leaky-wave antenna employing a tunable high impedance surface,'' *IEEE Trans. Antennas Propag.*, vol. 60, no. 11, pp. 5046–5055, Nov. 2012.

[18] Y. Geng, J. Wang, Y. Li, Z. Li, M. Chen, and Z. Zhang, ''Radiation pattern-reconfigurable leaky-wave antenna for fixed-frequency beam steering based on substrate-integrated waveguide,'' *IEEE Antennas Wireless Propag. Lett.*, vol. 18, no. 2, pp. 387–391, Feb. 2019.

[19] D. K. Karmokar, K. P. Esselle, and S. G. Hay, ''Fixed-frequency beam steering of microstrip leaky-wave antennas using binary switches,'' *IEEE Trans. Antennas Propag.*, vol. 64, no. 6, pp. 2146–2154, Jun. 2016.

[20] M. K. Mohsen, M. S. M. Isa, A. A. M. Isa, M. K. Abdulhameed, and M. L. Attiah, ''Achieving fixed-frequency beam scanning with a microstrip leaky-wave antenna using double-gap capacitor technique,'' *IEEE Antennas Wireless Propag. Lett.*, vol. 18, no. 7, pp. 1502–1506, Jul. 2019.

[21] T. Lou, X.-X. Yang, H. Qiu, Q. Luo, and S. Gao, ''Low-cost electrical beam-scanning leaky-wave antenna based on bent corrugated substrate integrated waveguide,'' *IEEE Antennas Wireless Propag. Lett.*, vol. 18, no. 2, pp. 353–357, Feb. 2019.

[22] D.M. Pozar, *Microwave Engineering*, 3rd ed. New York, NY, USA: Wiley, 2004.

[23] J. T. Williams, P. Baccarelli, S. Paulotto, and D. R. Jackson, ''1-D combline leaky-wave antenna with the open-stopband suppressed: Design considerations and comparisons with measurements,'' *IEEE Trans. Antennas Propag.*, vol. 61, no. 9, pp. 4484–4492, Sep. 2013.

[24] S. Otto, A. Rennings, K. Solbach, and C. Caloz, ''Transmission line modeling and asymptotic formulas for periodic leaky-wave antennas scanning through broadside,'' *IEEE Trans. Antennas Propag.*, vol. 59, no. 10, pp. 3695–3709, Oct. 2011.

[25] G. Valerio, S. Paulotto, P. Baccarelli, P. Burghignoli, and A. Galli, ''Accurate Bloch analysis of 1-D periodic lines through the simulation of truncated structures,'' *IEEE Trans. Antennas Propag.*, vol. 59, no. 6, pp. 2188–2195, Jun. 2011.

[26] S. Paulotto, P. Baccarelli, F. Frezza, and D. R. Jackson, ''A novel technique for open-stopband suppression in 1-D periodic printed leaky-wave antennas,'' *IEEE Trans. Antennas. Propag.*, vol. 57, no. 7, pp. 1894–1906, Jul. 2009.

[27] L. Liu, C. Caloz, and T. Itoh, ''Dominant mode leaky-wave antenna with backfire-to-endfire scanning capability,'' *Electron. Lett.*, vol. 38, no. 23, pp. 1414–1416, Nov. 2002.

BIN XI was born in Shanxi, China, in 1993. He received the B.Sc. degree in communication engineering from the Taiyuan University of Technology, Taiyuan, China, in 2016. He is currently pursuing the M.Eng. degree in electronics and information engineering from Sun Yat-sen University, Guangzhou, China.

His current research interest includes microstrip antenna design.

YUANXIN LI (M'08) was born in Guangzhou, China. He received the B.Sc. and Ph.D. degrees from Sun Yat-sen University, Guangzhou, China, in 2001 and 2006, respectively.

He was a Senior Research Assistant and also a Research Fellow with the State Key Laboratory of Millimeter Waves, City University of Hong Kong, Hong Kong, from 2006 to 2008 and in 2010, respectively. In 2008, he joined the Department of Electronics and Communication Engineering, Sun Yat-sen University, where he is currently an Associate Professor with the School of Electronics and Information Technology. He has published over 100 internationally refereed journal and conference papers, including 27 IEEE Transactions articles. His current research interests include microstrip leaky wave antenna and the applications of the periodic construction.

ZHIXI LIANG (M'18) was born in Huizhou, Guangdong, China, in 1989. He received the B.S. degree in electronics information science and technology and the Ph.D. degree in radio physics from Sun Yat-sen University, Guangzhou, China, in 2011 and 2016, respectively, where he holds a postdoctoral position.

His current research interests include microstrip patch antennas, microstrip magnetic dipole antennas, and endfire antennas.

SHAOYONG ZHENG (S'07–M'11–SM'17) was born in Fujian, China. He received the B.S. degree in electronic engineering from Xiamen University, Fujian, China, in 2003, and the M.Sc., M.Phil., and Ph.D. degrees in electronic engineering from the City University of Hong Kong, Kowloon, Hong Kong, in 2006, 2008, and 2011, respectively.

From 2011 to 2012, he was a Research Fellow with the Department of Electronic Engineering, City University of Hong Kong, where he was a Visiting Assistant Professor, from July to August 2013, from July to August 2014, and from July to August 2015. He is currently an Associate Professor with the School of Electronics and Information Technology, Sun Yat-sen University, Guangzhou, China, and the Deputy Director of the National Engineering Research Center of Mobile Communications (SYSU Branch). He has published over 100 internationally refereed journal and conference papers, including 48 IEEE Transactions articles. His research interests include microwave/millimeter wave components and evolutionary algorithms.

Dr. Zheng has served as a Technical Program Committee Member and a Session Organizer/Chair for a number of conferences (ICUWB, ACES, APCAP, iWEM, and so on.).

ZENGPING CHEN received the B.S. and Ph.D. degrees from the National University of Defense Technology, Changsha, China, in 1987 and 1994, respectively.

He is currently a Professor and a Ph.D. Supervisor with the School of Electronics and Communication Technology, Sun Yat-sen University. His current research interests include signal processing, radar systems, and automatic target recognition.

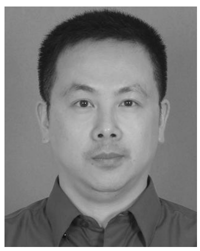

YUNLIANG LONG (M'01–SM'02) was born in Chongqing, China. He received the B.Sc., M.Eng., and Ph.D. degrees from the University of Electronic Science and Technology of China, Chengdu, China, in 1983, 1989, and 1992, respectively.

He was a Postdoctoral Research Fellow and an Associate Professor with the Department of Electronics, Sun Yat-sen University, Guangzhou, China, from 1992 to 1994. From 1998 to 1999, he was a Visiting Scholar with the Institut für Hochfrequenztechnik, RWTH Aachen University, Aachen, Germany. From 2000 to 2001, he was a Research Fellow with the Department of Electronics Engineering, City University of Hong Kong, Hong Kong. He is currently a Full Professor and the Head of the Department of Electronics and Communication Engineering, Sun Yat-sen University. He has authored or coauthored over 200 academic articles. His current research interests include antennas and propagation theory, EM theory in inhomogeneous lossy medium, computational electromagnetics, and wireless communication applications.

Dr. Long is a member of the Committee of Microwave Society of the Chinese Institute of Electronics and on the Editorial Board of the *Chinese Journal of Radio Science*. He is a Vice Chairman of the Guangzhou Electronic Industrial Association.